Hindawi Publishing Corporation
EURASIP Journal on Wireless Communications and Networking
Volume 2009, Article ID 912018, 8 pages
doi:10.1155/2009/912018

Research Article

Analytical SIR for Self-Organizing Wireless Networks

Abdurazak Mudesir,[1] Mathias Bode,[1] Ki Won Sung,[2] and Harald Haas[2]

[1] *School of Engineering and Science, Jacobs University Bremen, Campus Ring 12, 28759 Bremen, Germany*
[2] *Institute for Digital Communications, The University of Edinburgh, The Kings Buildings, Edingburgh EH9 3JL, UK*

Correspondence should be addressed to Abdurazak Mudesir, a.mudesir@jacobs-university.de

Received 14 May 2008; Revised 26 April 2009; Accepted 20 May 2009

Recommended by Visa Koivunen

The signal to interference ratio (SIR) in the presence of multipath fading, shadowing and path loss is a valuable parameter for studying the capacity of a wireless system. This paper presents a new generalized path loss equation that takes into account the large-scale path loss as well as the small-scale multipath fading. The probability density function (pdf) of the SIR for self-organising wireless networks with Nakagami-*m* channel model is analytically derived using the new path loss equation. We chose the Nakagami-*m* channel fading model because it encompasses a large class of fading channels. The results presented show good agreement between the analytical and Monte Carlo- based methods. Furthermore, the pdf of the signal to interference plus noise ratio (SINR) is provided as an extension to the SIR derivation. The analytical derivation of the pdf for a single interferer in this paper lays a solid foundation to calculate the statistics for multiple interferers.

1. Introduction

In a wireless communication environment characterized by dynamic channels, high influence of interference, bandwidth shortage and strong demand for quality of service (QoS) support, the challenge for achieving optimum spectral efficiency and high data rate is unprecedented. One of the bottlenecks in achieving these goals is modeling of the propagation environments [1]. The general aim of the work described in this paper is to assist in the derivation of the statistical properties of the SIR in a self-organizing wireless system, where network planning is minimal, without recourse to Monte Carlo simulations.

In a traditional system capacity studies, the pdf of the SIR has been determined through time-consuming Monte Carlo simulation or by only accounting for either the large-scale path loss [2] or multipath propagations [3], which are incomplete for studying realistic system deployment scenarios. This is primarily due to the complicated integrals involved in the derivation of the pdf of the SIR. Moreover, these studies usually assume strict hexagonal cell layout in order to simplify the calculation. The authors in [3] calculate the capacity of Nakagami multipath fading (NMF) channels assuming that the carrier-to-noise ratio (CNR) is gamma distributed. This assumption neglects the effects of shadowing and large- scale path loss. This paper presents an "exact" pdf derived from a model which is more closely related to a realistic deployment scenario.

With the results provided here, it is possible to calculate more precise capacity figures. Furthermore since the new path loss model takes into consideration the interaction of the large-scale path loss with the small-scale fading in which the cells are irregular shaped and arbitrarily positioned, this derivation is particularly suited to study the overall system performance of self-organizing networks. Self-organizing networks can be independent infrastructureless ad hoc networks or they can also be an extension to cellular networks, where different self-organizing mechanisms, such as intelligent relaying and adaptive cell sizing, are used to enhance coverage or capacity which are the two most important factors in wireless system planning [4]. The study of coverage and capacity relies on channel quality information. The channel quality can be captured by a single parameter, namely the received SIR. The SIR between two communicating nodes will typically decrease as the distance between the nodes increases, and will also depend on the signal propagation and interference environment. Hence modeling the SIR on the assumption of the strict hexagonal

cellular structure and the well-known path loss model that ignores the small-scale fading would not be applicable to self-configuring systems. Therefore analytical derivation of the pdf of SIR is a crucial step in constructing efficient system design.

Tellambura in [5] uses a characteristic function method to calculate the probability that the SIR drops below some predefined threshold (probability of outage) under the assumption of Nakagami fading. Zhan [6] also uses a similar characteristic function approach to derive outage probability for multiple interference scenario. These papers give a significant advantage in reducing the computational complexity involved in solving multiple integrals in SIR computation. But, a major shortcoming of these and other similar papers [7] is that, only the small-scale fading or large-scale fading is considered in analytically deriving the SIR statistics.

To the best of our knowledge, there has not been any work done to analytically derive the pdf of the SIR using the three mutually independent phenomena: multipath fading, shadowing and path loss together.

The rest of this paper is organized as follows. In Section 2 the system model considered is presented and in Section 3 the analytical derivation is described in detail. Section 4 provides the numerical and the simulation results. Section 5 concludes the paper.

2. System Model and Problem Formulation

For simplicity the cell layout used to derive the pdf of the SIR assumes circular cells, as shown in Figure 1, with maximum cell radius R_c instead of hexagonal cells. The cells are randomly positioned resulting in potentially overlapping cells. Randomly positioned cells model an important network scenario, which lacks any frequency planning as a result of self-configuring and self-organising networks, cognitive radio and multihop ad hoc communication. A receiver experiences interference from transmitters within its accessibility radius, R_{ac}. Due to propagation path loss, a transmitter outside the accessibility region incurs only a negligible interference. Since the aim is to model a realistic interference limited environment, the receiver accessibility radius is taken to be much greater than the cell radius, that is, $R_{ac} \gg R_c$. The dashed line in Figure 1 represents the interference link between transmitter, Tx y, and receiver, Rx z while the solid line shows the desired link between transmitter Tx x and receiver Rx z and vise versa. Throughout the paper omni directional antennas with unity gains are considered. The pdf is calculated assuming one interfering user. The results obtained can be extended to multiple interfering users by using laguerre polynomials to approximate the multiple integration resulting from the multiple interfering users. The analytical derivation of SIR for multiple interference is under study.

3. Analytical Derivation of the pdf of the SIR

In an interference limited environment, the received signal quality at a receiver is typically measured by means of

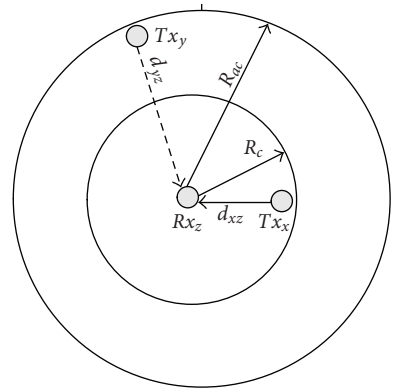

Figure 1: Model to drive the pdf of the SIR from a single neighboring cell.

achieved SIR, which is the ratio of the power of the wanted signal to the total residue power of the unwanted signals. let P_t and P_r denote the transmit and received power respectively. Let G denote the path gain and G_{yz} is the link gain between the interfering transmitter y and the receiver z. For the purpose of clarity, unless otherwise stated, a single subscript x, y or z specifies the node, and a double subscript such as xz specifies the link between node x and node z. A node is any entity, mobile station (MS) or base station (BS), that is, capable of communicating. For a single interfering user y depicted in Figure 1:

$$\mathrm{SIR}_z = \frac{P_{tx}G_{xz}}{P_{ty}G_{yz}}. \tag{1}$$

Assuming fixed and constant transmit powers, $P_{tx} = P_{ty} = \text{const}$, (1) simplifies to:

$$\mathrm{SIR}_z = \frac{G_{xz}}{G_{yz}}, \tag{2}$$

$$L = \frac{1}{G} \Longrightarrow \mathrm{SIR}_z = \frac{L_{yz}}{L_{xz}} \tag{3}$$

where L_{xz}, L_{yz} are the path losses between transmitter Tx x and receiver Rx z and Tx y and Rx z respectively.

Like the gain parameter G, the loss parameter L incorporates effects such as propagation loss, shadowing and multipath fading.

The generalized path loss model for the cross-layer environment is given by

$$L = \underbrace{C\left(\frac{d}{d_0}\right)^{\gamma} e^{(\beta\xi)}}_{\text{large-scale path loss}} \cdot \underbrace{\frac{1}{|H(f)|}}_{\text{small-scale path loss}} \tag{4}$$

where $C = \hat{C}/\tilde{C}$ is an environment specific constant, $\hat{C}$ the constant corresponding to the desired link while $\tilde{C}$ corresponds to the interference link. The distance d_0 is a constant and d is a random variable, γ is the path loss exponent, ξ is the random component due to shadowing,

$\beta = \ln(10)/10$ and $|H(f)|$ is a random variable modeling the channel envelop.

The commonly used path loss equation [2] only accounts for the large-scale path loss with regular cell deployment scenarios, which is incomplete for studying self-organizing networks. The new path loss model proposed in this paper takes into consideration the interaction of the large-scale path loss as well as the small-scale fading. This model is particularly important in studying the performance of self-organizing self-configuring networks.

For the interference scenario described in the system model, the path loss for the desired path and the path loss between the interfering transmitter y and the receiver z (interfering link) are

$$L_{xz} = \widetilde{C} d_{xz}^{\gamma_{xz}} \mathrm{e}^{(\beta\xi_{xz})} \frac{1}{|H_{xz}|}, \tag{5}$$

$$L_{yz} = \widehat{C} d_{yz}^{\gamma_{yz}} \mathrm{e}^{(\beta\xi_{yz})} \frac{1}{\left|H_{yz}\right|}, \tag{6}$$

where L_{xz} is the path loss model for the desired link and L_{yz} is the path loss model for the interfering link. d_{yz} models the distance between the interference causing transmitter, x, and the victim receiver y. γ_{yz} and γ_{xz} are the path loss exponents, ξ_{xz} and ξ_{yz} are Gaussian distributed random variables modeling the shadow fading with each zero mean and variances v_{xz}^2 and v_{yz}^2 respectively, and $|H_{xz}|$ and $|H_{yz}|$ are the channel envelope modeling the channel fading. For the purpose of clarity, the time and frequency dependencies are not shown. The channel envelope is assumed to follow the Nakagami-m distribution. Nakagami distribution is a general statistical model which encompasses Rayleigh distribution as a special case, when the fading parameter $m = 1$, and also approximates the Rician distribution very well. In addition, Nakagami-m distribution will also provide the flexibility of choosing different distributions for the desired link and interfering link, such as the Rayleigh for the channel envelope of the desired link, and Rician for the interfering link, or vice versa.

Using (3) and (5), the SIR can be given as

$$\mathrm{SIR} = \frac{C d_{yz}^{\gamma_{yz}} \mathrm{e}^{(\beta\xi_{yz})} |H_{xz}|}{d_{xz}^{\gamma_{xz}} \mathrm{e}^{(\beta\xi_{xz})} \left|H_{yz}\right|}. \tag{7}$$

From (7), the SIR has six random variable components, $\Phi_{xz} = d_{xz}^{\gamma_{xz}}$, $\Phi_{yz} = d_{yz}^{\gamma_{yz}}$, $\Lambda_{xz} = \mathrm{e}^{(\beta\xi_{xz})}$, $\Lambda_{yz} = \mathrm{e}^{(\beta\xi_{yz})}$, $|H_{xz}|$ and $|H_{yz}|$. In order to analytically derive the pdf of the SIR, the pdf of the individual components and also their ratios and products need to be determined first.

The following two formulas provide the basic framework for the analysis and will be used throughout the derivation. Given two independent random variables X and Y the pdf of their product $f_Z(z)$ where $Z = XY$ is

$$f_Z(z) = \int f_X\left(\frac{z}{x}\right) f_Y(x) \left(\frac{1}{|x|}\right) dx. \tag{8}$$

Given two independent random variables Y and X the pdf of their ratio $f_Z(z)$ where $Z = Y/X$ is

$$f_Z(z) = \int f_X(x) f_Y(zx) |x| dx. \tag{9}$$

3.1. pdf of the Ratio of the Propagation Loss. It is assumed that the distance between the interfering transmitter and the receiver, d_{yz}, is uniformly distributed up to a maximum distance of R_{ac}, and that the distance between an interfering transmitter and intended receiver, d_{xz}, is uniformly distributed up to a maximum distance of R_c. Therefore Φ_{xz} and Φ_{yz} are both functions of random variables, and their pdfs can be derived using the following random variable transformation [8]:

$$p(\theta) = \left.\frac{p(\delta)}{|d(\theta)/d(\delta)|}\right|_{\delta=\mathrm{F}^{-1}(\theta)}, \tag{10}$$

where θ and δ are random variables with pdfs $p(\theta)$ and $p(\delta)$ respectivly, and where θ is a function of $\mathrm{F}(\delta)$, $d(\theta)$ and $d(\delta)$ are the first derivatives of θ and δ respectively.

The mathematical representation of the pdfs of d_{xz} and d_{yz} are

$$\begin{aligned} f_{D_{xz}}(d_{xz}) &= \frac{2d_{xz}}{R_{\mathrm{c}}^2}, \quad 0 < d_{xz} \le R_{\mathrm{c}}, \\ f_{D_{yz}}\left(d_{yz}\right) &= \frac{2d_{yz}}{R_{\mathrm{ac}}^2}, \quad 0 < d_{yz} \le R_{\mathrm{ac}}. \end{aligned} \tag{11}$$

Let $f_{\Phi_{xz}}(\phi_{xz})$ and $f_{\Phi_{yz}}(\phi_{yz})$ denote the pdfs of Φ_{xz} and Φ_{yz}. Then employing the transformation (10), $f_{\Phi_{xz}}(\phi_{xz})$ and $f_{\Phi_{yz}}(\phi_{yz})$ are derived as

$$\begin{aligned} f_{\Phi_{xz}}(\phi_{xz}) &= \frac{2{\phi_{xz}}^{2/\gamma_{xz}-1}}{R_{\mathrm{c}}^2 \gamma_{xz}} \quad 0 < \phi_{xz} \le R_{\mathrm{c}}^{\gamma_{xz}}, \\ f_{\Phi_{yz}}\left(\phi_{yz}\right) &= \frac{2{\phi_{yz}}^{2/\gamma_{yz}-1}}{R_{\mathrm{ac}}^2 \gamma_{yz}} \quad 0 < \phi_{yz} \le R_{\mathrm{ac}}^{\gamma_{yz}}. \end{aligned} \tag{12}$$

Using (9), the pdf of the ratio of the propagation loss, $\Phi = \Phi_{yz}/\Phi_{xz}$, is found to be

$$f_\Phi(\phi) = \begin{cases} \Upsilon \phi^{2/\gamma_{yz}-1}, & \text{for } 0 < \phi \le \varsigma, \\ \widetilde{\Upsilon} \phi^{-2/\gamma_{xz}-1}, & \text{for } \varsigma < \phi < \infty, \end{cases} \tag{13}$$

where $\varsigma = R_{\mathrm{ac}}^{\gamma_{yz}}/R_{\mathrm{c}}^{\gamma_{xz}}$, $\Upsilon = 2R_{\mathrm{c}}^{2(\gamma_{xz}/\gamma_{yz})}/R_{\mathrm{ac}}^2(\gamma_{yz}+\gamma_{xz})$ and $\widetilde{\Upsilon} = 2R_{\mathrm{ac}}^{2(\gamma_{yz}/\gamma_{xz})}/R_{\mathrm{c}}^2(\gamma_{yz}+\gamma_{xz})$.

The next step to derive the pdf of the SIR is to find the pdf of the ratio of the lognormal shadowing.

3.2. pdf of the Ratio of the Lognormal Shadowing. Given a normally distributed random variable X with mean μ and variance σ^2, and a real constant c, the product cX is known to follow a normal distribution with mean $c\mu$ and a variance $c^2\sigma^2$ and e^X has a log normal distribution. Since ξ_{xz} is normally distributed with mean μ and variance σ^2,

$\Lambda_{xz} = e^{(\beta\xi_{xz})}$ is a lognormal distributed random variable with mean μ_{xz} and variance $\nu_{xz}^2 = \beta^2{\sigma_{xz}}^2$ expressed in terms of the normally distributed ξ_{xz}, while the mean and variance of $\Lambda_{yz} = e^{(\beta\xi_{yz})}$ are μ_{yz} and $\nu_{yz}^2 = \beta^2\sigma_y z^2$, respectively,

$$f_{\Lambda_{xz}}(\lambda_{xz}) = \frac{e^{-1/2\left(\ln(\lambda_{xz})-\mu_{xz}\right)^2/{\nu_{xz}}^2}}{\lambda_{xz}\nu_{xz}\sqrt{2\pi}}, \quad 0 \le \lambda_{xz} < \infty,$$
$$f_{\Lambda_{yz}}\left(\lambda_{yz}\right) = \frac{e^{-1/2\left(\ln\left(\lambda_{yz}\right)-\mu_{yz}\right)^2/{\nu_{yz}}^2}}{\lambda_{yz}\nu_{yz}\sqrt{2\pi}}, \quad 0 \le \lambda_{yz} < \infty. \tag{14}$$

Since the ratio of two independent lognormal random variables is itself a lognormal distributed random variable. Therefore the pdf of $\Lambda = \Lambda_{yz}/\Lambda_{xz}$ is

$$f_\Lambda(\lambda) = \frac{e^{-1/2\left(\ln(\lambda)-\mu\right)^2/\sigma^2}}{\lambda\sigma\sqrt{2\pi}}, \quad 0 \le \lambda < \infty, \tag{15}$$

where

$$\sigma = \beta\sqrt{\nu_{xz} + \nu_{yz}}, \quad \mu = 0. \tag{16}$$

The last components remaining from (7) are the random variables modeling the channel envelop and their ratios.

3.3. pdf of the Ratio of the Channel Envelope. In order to accommodate different channel fading distributions, Nakagami-m distribution was used to model the channel envelope. Nakagami-m distribution is the most general of all distribution known until now [9].

The Nakagami-m pdf is given by

$$f_{|H_{xz}|}(h_{xz}) = \frac{2}{\Gamma(m_{xz})}\left(\frac{m_{xz}}{\Omega_{xz}}\right)^{m_{xz}} {h_{xz}}^{2m_{xz}-1} e^{-m_{xz}{h_{xz}}^2/\Omega_{xz}}, \quad 0 \le h_{xz} < \infty \tag{17}$$

$$f_{|H_{yz}|}\left(h_{yz}\right) = \frac{2}{\Gamma\left(m_{yz}\right)}\left(\frac{m_{yz}}{\Omega_{yz}}\right)^{m_{yz}} {h_{yz}}^{2m_{yz}-1} e^{-m_{yz}{h_{yz}}^2/\Omega_{yz}}, \quad 0 \le h_{yz} < \infty \tag{18}$$

where $m \ge 1/2$ represents the fading figure, $\Omega = E(x^2)$ is the average received power and $\Gamma(\cdot)$ is the gamma function given as

$$\Gamma(m) = \int_0^\infty x^{m-1}e^{-x}dx. \tag{19}$$

Using (8) and (9) the pdf of the ratio of Nakagamai channel evelopes, $\Psi = |H_{xz}|/|H_{yz}|$ is

$$f_\Psi(\psi) = M\frac{\psi^{2m_{xz}-1}}{\left(m_{yz}/2\sigma_{xz}^2 + (m_{xz}/2\sigma_{yz}^2)\psi^2\right)^{\left(m_{yz}+m_{xz}\right)}}, \quad 0 \le \quad \psi < \infty \tag{20}$$

where

$$M = \frac{2\Gamma\left(m_{yz}+m_{xz}\right)}{\Gamma\left(m_{yz}\right)\Gamma(m_{xz})}\left(\frac{m_{yz}}{\Omega_{xz}}\right)^{m_{yz}}\left(\frac{m_{xz}}{\Omega_{yz}}\right)^{m_{xz}} \tag{21}$$

for $m_{xz} = m_{yz} = 1$ the ratio of the Nakagami-distributed channel is the same as the ratio of two independent Rayleigh distributed envelopes.

The final step in the derivation of the pdf of the SIR is deriving the product of the above obtained pdfs.

3.4. pdf of the SIR. As shown in (7) the pdf of the SIR is the product of the three individual random variables, Φ, Λ and Ψ. Using the equations presented so far, the final pdf of the SIR is presented in (22):

$$f_{\mathrm{SIR}}(\zeta) = M\zeta^{2m_{xz}-1} \times \int_0^\infty \frac{A_1\chi^{q_1}\left(\mathrm{erf}\left(\left(2/\gamma_{yz}\right)\sigma^2 + \ln\left(\chi/(\mathcal{A})\right)/\sqrt{2}\sigma\right)-1\right)}{\left((m_{yz}/\Omega_{xz} + m_{xz}/\Omega_{yz})\left(\zeta/\chi\right)^2\right)^{\left(m_{yz}+m_{xz}\right)}} + \frac{B_1\chi^{q_2}\left(-1-\mathrm{erf}\left(\left(-2/\gamma_{xz}\right)\sigma^2+\ln\left(\chi/(\mathcal{A})\right)/\sqrt{2}\sigma\right)\right)}{\left((m_{yz}/\Omega_{xz}+m_{xz}/\Omega_{yz})\left(\zeta/\chi\right)^2\right)^{\left(m_{yz}+m_{xz}\right)}}d\chi \tag{22}$$

where $q_1 = (2/\gamma_{yz}) - 2m_{yz} - 1$, $q_2 = (-2/\gamma_{xz}) - 2m_{yz} - 1$, and $\mathcal{A}$ denotes $R_{\mathrm{ac}}^{\gamma_{yz}}/R_{\mathrm{c}}^{\gamma_{xz}}$:

$$A_1 = \frac{-2R_{\mathrm{c}}^{2(\gamma_{xz}/\gamma_{yz})}/R_{\mathrm{ac}}^2\left(\gamma_{yz}+\gamma_{xz}\right)}{2}e^{\left(2/\gamma_{yz}^2\right)\sigma^2},$$
$$B_1 = \frac{-2R_{\mathrm{ac}}^{2(\gamma_{yz}/\gamma_{xz})}/R_{\mathrm{c}}^2\left(\gamma_{yz}+\gamma_{xz}\right)}{2}e^{\left(2/\gamma_{xz}^2\right)\sigma^2}. \tag{23}$$

The final equation does not have a closed form solution but it is possible to solve the integration using numerical methods.

4. Signal to Interference and Noise Ratio

In case of an environment that is is not interference limited, the (signal to interference and noise ratio) SINR is required to fully describe the communication channel. SINR can easily be found by modifying the SIR equation given in (1):

$$\mathrm{SINR}_z = \frac{G_{xz}}{G_{yz}+N}, \tag{24}$$

where N is the random variable modeling the Gaussian noise with mean $m_N = 0$ and a standard deviation of σ_N. By applying the generalized path loss equation in (4), SINR at the receiver Rx z is given by:

$$\mathrm{SINR}_z = \frac{|H_{xz}|/d_{xz}^{\gamma_{xz}}e^{\left(\beta\xi_{xz}\right)}}{\left(\left|H_{yz}\right|/d_{yz}^{\gamma_{yz}}e^{\left(\beta\xi_{yz}\right)}\right)+N}, \tag{25}$$

where the pdfs of the individual random variables are given in the previous section. Let $\Theta_{xz} = \Phi_{xz}\Lambda_{xz} = {d_{xz}}^{\gamma_{xz}}e^{(\beta\xi_{xz})}$

which are derived in the previous section. The pdf of Θ_{xz}, $f_{\Theta_{xz}}(\theta_{xz})$, is given as

$$f_\Theta(\theta_{xz}) = \int f_\Phi\left(\frac{\theta_{xz}}{\lambda_{xz}}\right) f_{\Lambda_{xz}}(\lambda_{xz})\left(\frac{1}{|\lambda_{xz}|}\right) d\lambda_{xz}$$

$$f_\Theta(\theta_{xz}) = \int_{\theta_{xz}/R_c^2}^{\infty} \frac{2(\theta_{xz}/\lambda_{xz})^{2/\gamma_{xz}-1}}{R_c^2\gamma_{xz}} \frac{e^{-1/2\,(\beta(\ln(\lambda_{xz})-\mu)^2/\nu_{xz}{}^2)}}{\lambda_{xz}\nu_{xz}\sqrt{2\pi}} \times \frac{1}{\lambda_{xz}} d\lambda_{xz}$$

$$f_\Theta(\theta_{xz}) = D\left(1 - \frac{\operatorname{erf}\left(2\nu_{xz}{}^2 - \gamma_{xz}m_{xz} + \gamma_{xz}\log\left(\theta_{xz}/R_c^{\gamma_{xz}}\right)\right)}{\sqrt{(2)\gamma_{xz}\nu_{xz}}}\right) \tag{26}$$

where $D = (e^{(2\nu_{xz}{}^2 - 2\gamma_{xz}m_{xz})/\gamma_{xz}{}^2}/R_c^2\gamma_{xz})\theta_{xz}{}^{2/(\gamma_{xz}-1)}$.

The next step in the derivation is to find the pdf of the path loss of the desired link by utilizing (9) and (17). Let $S = |H_{xz}|/d_{xz}^{\gamma_{xz}} e^{(\beta\xi_{xz})}$ be the random variable denoting the path loss of the desired link. The pdf of S is given as

$$f_S(s) = K\int_0^\infty h_{xz}{}^{2m_{xz}} e^{-m_{xz}h_{xz}{}^2/\Omega_{xz}} \times \left(1 - \frac{\operatorname{erf}\left(2\nu_{xz}{}^2 - \gamma_{xz}m_{xz} + \gamma_{xz}\log\left(sh_{xz}/R_c^{\gamma_z xz}\right)\right)}{\sqrt{(2)\gamma_{xz}\nu_{xz}}}\right) dh_{xz}, \tag{27}$$

where $K = (2/\Gamma(m_{xz}))(m_{xz}{}^2/\Omega_{xz})D$.

The pdf of the path loss of the interference path denoted by the random variable $I = |H_{yz}|/d_{yz}^{\gamma_{yz}} e^{(\beta\xi_{yz})}$ is give as

$$f_I(i) = \hat{K}\int_0^\infty h_{yz}{}^{2m_{yz}} e^{-m_{yz}h_{yz}{}^2/\Omega_{yz}} \times \left(1 - \frac{\operatorname{erf}\left(2\nu_{yz}{}^2 - \gamma_{yz}m_{yz} + \gamma_{yz}\log\left(ih_{yz}/R_{\mathrm{TV}}^{\gamma_{yz}}\right)\right)}{\sqrt{(2)\gamma_{yz}\nu_{yz}}}\right) dh_{yz}, \tag{28}$$

where $\hat{K} = (2/\Gamma(m_{yz}))(m_{yz}{}^2/\Omega_{yz})D$.

In order to find the pdf of the interference plus noise, $I + N$, it is assumed that interference is independent of noise. The pdf of the sum of two independent random variables U and V, each of which has a probability density function, is the convolution of their individual density functions

$$f_{U+V}(z) = \int f_U(z-x) f_V(x) dx, \tag{29}$$

therefore the pdf of $I + N$, $f_{I+N}(z)$ is given by:

$$f_{I+N}(z) = \int_0^\infty f_I(z-x) f_N(x) dx, \tag{30}$$

where $f_N(x) = e^{-(1/2)(x/\sigma_N)^2}/(\sqrt{2\pi}\,\sigma_N)$. Utilizing (9), the pdf of the SINR is given by

$$f_{\mathrm{SINR}}(\nu) = \int_0^\infty f_{I+N}(z) f_S(\nu z) z dz. \tag{31}$$

For the special case where the noise approaches zero, the pdf of the noise is represented as delta function or also known as, a unit impulse function, around zero. Therefore (30) can be rewritten as

$$f_{I+N}(z) = \int_0^\infty f_I(z-x) f_N(x) dx = \int_0^\infty f_I(z-x)\delta(x) dx = f_I(z). \tag{32}$$

Thus

$$f_{\mathrm{SINR}}(\nu) = \int_0^\infty f_{I+N}(z) f_S(\nu z) z dz = \int_0^\infty f_I(z) f_S(\nu z) z dz \tag{33}$$

by the definition given in (9), the $f_{\mathrm{SINR}}(\nu)$ given in (33) is the pdf of the SIR(S/I). Therefore, when the noise approaches to zero, the pdf of the SINR given in (31) reduces to the pdf of SIR given in (22).

This sub-section has presented the pdf of the SINR as an extension to the pdf of the SIR. To validate the analytically derived SINR pdf, it is important to show that the core derivation, SIR derivation, is valid. The next sub-section validates the derivation through comparative numerical simulations of the SIR. The results presented were obtained using the adaptive Simpson quadrature numerical integration of the SIR.

5. Results and Discussion

Monte Carlo simulations are carried out in order to validate the analytically derived pdf results. Figures 2 and 3 show plots of the pdf of the SIR $f_{\mathrm{SIR}}(\zeta)$ for different scenarios. The results presented in Figures 2–4 show that the analytical pdf is in good agreement with the Monte Carlo simulation. The parameters used for the shadow fading, channel standard deviation and path loss exponents reflect a realistic deployment scenario for users moving at a speed of 25 to 40 km/h [10]. All simulations assume a channel envelope with a Nakagami-m distribution with different m parameter, which corresponds to different fading scenario. These parameters are summarized in Tables 1, 2, and 3.

Figure 2 depicts three different plots depending on the R_{ac}/R_c. As the cell radius R_c increases there is a significant cell overlap leading to high mean value of interference which in turn leads to lower SIR mean value. Therefore, as the ratio of the cell radius to the accessibility radius approaches to one, the pdf is skewed towards smaller SIR. These plots show that the node with the lowest cell radius, $R_c = 100\,m$, has the highest SIR mean.

Figure 3 shows the effect of different environments on the pdf of the SIR. The figure presents plots from an ad hoc free space outdoor deployment with line of sight scenario on the desired link, $\gamma = 2$ and $m = 3$, to the most severe non-line-of-sight scenario of obstructed indoor (in building) environment, $\gamma = 4$ and $m = 0.5$. The radius of the cell, R_c, has been set to 100 m, which is considered a good

Table 1: System parameters for Figure 2 (varying cell and accessability radius).

Parameter	Values
R_c	100 m
R_{ac}	500 m
ν_{xz}	6 dB
ν_{yz}	10 dB
γ_{xz}	2
γ_{yz}	4
m_{xz}	5
m_{yz}	0.5
Ω_{xz}	4 dB
Ω_{yz}	6 dB

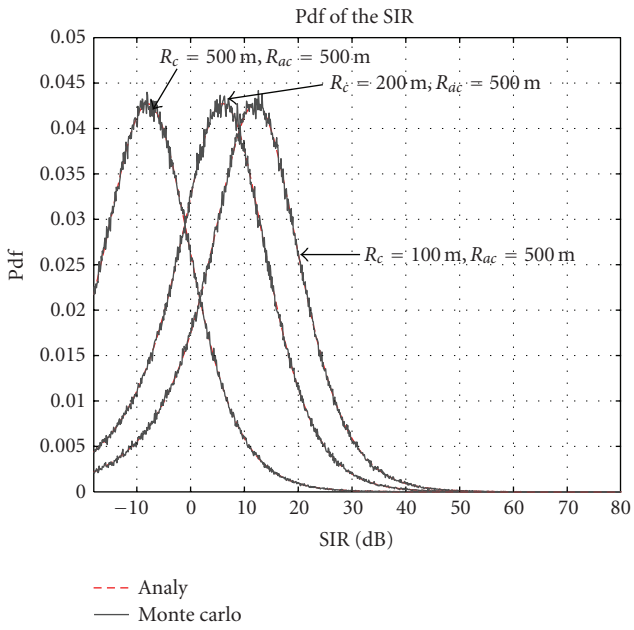

Figure 2: Plots of the pdf of the SIR for different values of cell radius.

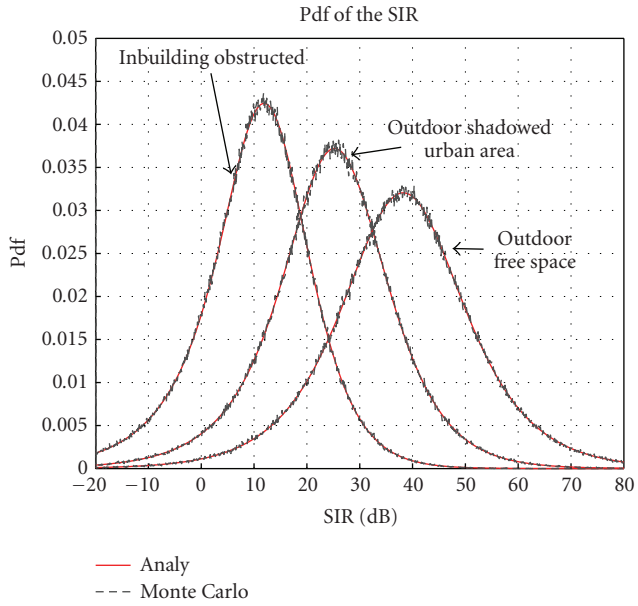

Figure 3: Plots of the pdf of the SIR for different environments.

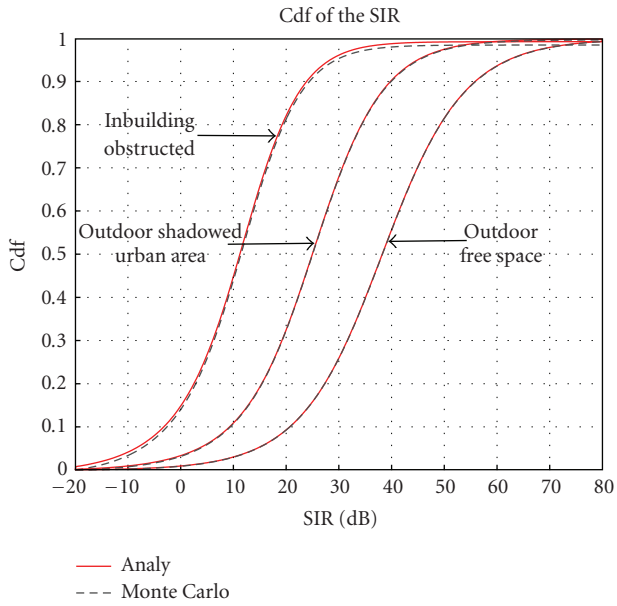

Figure 4: Plots of the pdf of the SIR for different environments .

configuration example for *ad hoc* networks. The accessability radius, R_{ac} is assumed to be 500 m. The results illustrate that the node with the best line-of-sight (LOS) link, $\gamma_{xz} = 2$ and $\gamma_{yz} = 4$, has the highest mean SIR value and the biggest variance or spread. While the node with the most obstructed inbuilding environment, exhibits the lowest mean and the smallest variance or spread of all. These can be attributed to the higher interference contribution of interfering node in NLOS link than those in LOS condition.

Figure 4 present the cumulative density function of the SIR. The simulation parameters are summarized in Table 3. From Figure 4 it can be observed that for a target SIR of 25 dB, being a reasonable assumption for 64-QAM modulation, the probability that the SIR exceeds the target SIR in the most severe non-line-of-sight scenario of obstructed indoor (in building) environment is about 10% resulting in a high outage probability enforcing the use of lower order modulation schemes. On the other hand, for the link with best LOS condition of outdoor free space environment the probability that the SIR exceeds the target SIR is 85% allowing the use of higher order modulation. Therefore from the results in Figure 4, it can be deducted that the analytical work presented in the paper can be used in determining the boundaries for varying the modulation order. A similar work of determining the boundaries for adaptive modulation was presented by Goldsmith et al. and M.-S. Alouini [11] assuming Nakagami distribution thus ignoring the shadowing effect, the pdf presented here can be used to extend the results presented in [11].

Table 2: System parameters for Figure 3.

Parameter	Inbuilding obstructed	Outdoor shadowed urban	Outdoor free space
R_c	100 m	100 m	100 m
R_{ac}	500 m	500 m	500 m
ν_{xz}	10 dB	8 dB	10 dB
ν_{yz}	10 dB	10 dB	10 dB
γ_{xz}	4	3	4
γ_{yz}	4	4	4
m_{xz}	3	1	0.5
m_{yz}	0.5	0.5	0.5
Ω_{xz}	4 dB	4 dB	4 dB
Ω_{yz}	6 dB	4 dB	6 dB

Table 3: System parameters for Figure 4.

Parameter	Inbuilding obstructed	Outdoor shadowed urban	Outdoor free space
R_c	100 m	100 m	100 m
R_{ac}	500 m	500 m	500 m
ν_{xz}	10 dB	8 dB	10 dB
ν_{yz}	10 dB	10 dB	10 dB
γ_{xz}	4	3	4
γ_{yz}	4	4	4
m_{xz}	3	1	0.5
m_{yz}	0.5	0.5	0.5
Ω_{xz}	4 dB	4 dB	4 dB
Ω_{yz}	6 dB	4 dB	6 dB

6. Conclusion

The main contribution of this paper is the derivation of the pdf of the SIR in a self-organizing wireless system, where network planning is minimal, without recourse to Monte Carlo simulations. The derivation was carried out using a generalized path loss model that accounts for both large and small- scale path loss. The use of Nakagami-m distribution for the fading channel gives the flexibility to use Rayleigh or different channel fading models for the desired and interfering links. The results obtained show excellent agreement with the Monte Carlo based results. The SIR derivation was in turn used to derive the pdf of the SINR. The SINR derivation is important in non-interference limited environment. These derivations can be further used in applications where the knowledge of SIR is necessary, such as link adaptation algorithms and cognitive radio design. The analytical derivation of the pdf from a single interferer in this paper lays a solid foundation to calculate the statistics from multiple interferers.

Acknowledgments

This work is supported by DFG Grant HA 3570/1-2 within the program SPP-1163, TakeOFDM. Harald Haas acknowledges the Scottish Funding Council's support of his position within the Edinburgh Research Partnership in Engineering and Mathematics between the university of Edinburgh and Heriot Watt university. This work was presented in part at the IEEE International Symposium of Personal, Indoor and Mobile Radio Communications (PIMRC) 2008, Cannes,France.

References

[1] Z. Yun and M. F. Iskander, "Progress in modeling challenging propagation environments," in *Proceedings of the IEEE Antennas and Propagation Society International Symposium (APS '04)*, vol. 4, pp. 3637–3640, Anaheim, Calif, USA, 2004.

[2] T. S. Rappaport, *Wireless Communications: Principles and Practice*, Prentice-Hall PTR, Englewood Cliffs, NJ, USA, 2nd edition, 2001.

[3] M.-S. Alouini and A. Goldsmith, "Capacity of Nakagami multipath fading channels," in *Proceedings of the IEEE Vehicular Technology Conference (VTC '97)*, vol. 1, pp. 358–362, Phoenix, Ariz, USA, May 1997.

[4] A. Spilling, A. Nix, M. Beach, and T. Harrold, "Self-organisation in future mobile communications," *IEE Electronics & Communication Engineering Journal*, vol. 12, pp. 133–147, 2000.

[5] C. Tellambura, "Cochannel interference computation for arbitrary Nakagami fading," *IEEE Transactions on Vehicular Technology*, vol. 48, no. 2, pp. 487–489, 1999.

[6] Q. T. Zhang, "Outage probability in cellular mobile radio due to Nakagami signal and interferers with arbitrary parameters," *IEEE Transactions on Vehicular Technology*, vol. 45, no. 2, pp. 364–372, 1996.

[7] M. Zorzi, "On the analytical computation of the interference statistics with applications to the performance evaluation of mobile radio systems," *IEEE Transactions on Communications*, vol. 45, no. 1, pp. 103–109, 1997.

[8] A. Papoulis, *Probability, Random Variables, and Stochastic Processes*, McGraw-Hill, New York, NY, USA, 3rd edition, 1991.

[9] M. Nakagami, "The m-distribution: a general formula of intensity distribution," in *Statistical Methods of Radio Wave Propagation*, W. C. Hoffman, Ed., pp. 3–36, Pergamon, New York, NY, USA, 1960.

[10] I. K. Eltahir, "The impact of different radio propagation models for mobile ad hoc NETworks (MANET) in urban area environment," in *Proceedings of the 2nd International Conference on Wireless Broadband and Ultra Wideband Communications (AusWireless '07)*, p. 30, Sydney, Australia, August 2007.

[11] M.-S. Alouini and A. J. Goldsmith, "Adaptive modulation over Nakagami fading channels," *Wireless Personal Communications*, vol. 13, no. 1, pp. 119–143, 2000.